Journal of Aerosol Science 46 (2012) 1–6

Contents lists available at SciVerse ScienceDirect

Journal of Aerosol Science

journal homepage: www.elsevier.com/locate/jaerosci

A study of ejection modes for pulsed-DC electrohydrodynamic inkjet printing

M.W. Lee [a], D.K. Kang [a], N.Y. Kim [a], H.Y. Kim [a], S.C. James [b], S.S. Yoon [a,*]

[a] Department of Mechanical Engineering, Korea University, Seoul 136-713 Korea
[b] Thermal/Fluid Science & Engineering, Sandia National Laboratories, P.O. Box 969, Livermore, CA 94551, USA

ARTICLE INFO

Article history:
Received 23 August 2011
Received in revised form
11 October 2011
Accepted 15 November 2011
Available online 1 December 2011

Keywords:
Electrohydrodynamic (EHD)
Drop-on-demand (DOD)
Pulsed DC
Microdripping mode

ABSTRACT

For electrohydrodynamic-driven drop-on-demand printing techniques, either continuous- or pulsed-DC voltages can generate drops. To generate uniform micro-drops for high-resolution printing, the pulsed-DC voltage method is superior to continuous-DC voltage methods because of its controllability. Voltage amplitude and duration (or duty cycle or relaxation time, τ) are the primary parameters affecting the performance of drop-generation or ejection. When charge accumulates on the fluid meniscus at the nozzle, a drop is ejected. Charge density is the product of voltage (amplitude) and duration. In theory, charge densities from low-amplitude, long-duration voltages are equivalent to those of large amplitude and short duration. However, we demonstrate that drop-ejection mode differs significantly, despite equivalent products when voltage amplitude and duration change. At various voltage amplitudes and durations, four ejection main modes are identified: micro-dripping, spindle, string-jet, and spray modes. Longer voltage durations yield excessively large, spindle, string-jet, and spray modes. Conversely, no ejection is observed for short voltage durations. The microdripping mode, most desirable for uniform and high-resolution printing, appears for the narrowed range of duration under given pulsed-voltage. The identification map has been constructed for these modes; this map can be used as a guide-line to yield a stable microdripping mode for high quality printing.

1. Introduction

Micro- and nano-patterning with electrohydrodynamic (EHD) inkjets have been well demonstrated, but issues remain with high-resolution printing (Wu et al., 2006; Wu & Russel, 2009). Advantages of an EHD inkjet include its ability to generate controlled, nano-scale drops while maintaining accurate targeting under a directional electro-magnetic field; this is often referred to as high resolution drop-on-demand (DOD) (Wu & Russel, 2009). EHD inkjets show promise for applications such as thin-film deposition, pharmaceutical particle production, encapsulation, spray forming, direct writing, etc. (Jaworek & Sobczyk, 2008; Salata, 2005; Singh et al., 2010; Wu & Russel, 2009; Yurteri et al., 2010). EHD inkjets are especially useful for nano-printing or patterning for industrial applications including manufacture of semi-conductors, visual displays, and solar cell electrodes; it can both line and dot print in 2D or 3D on various substrates (Eom et al., 2008, 2009; Ishida et al., 2007; Krebs, 2009). Its non-contact printing precludes damage to fragile substrates.

While there is a wealth of literatures on EHD printing techniques, details on voltage frequency control (pulse duration and amplitude) have not yet been well addressed. There are two primary EHD printing techniques: continuous- and

* Corresponding author. Tel.: +82 2 3290 3376; fax: +82 2 926 9290.
E-mail address: skyoon@korea.ac.kr (S.S. Yoon).

0021-8502/$ - see front matter © 2011 Elsevier Ltd. All rights reserved.
doi:10.1016/j.jaerosci.2011.11.002

pulsed-DC voltage. Voltage is supplied to the conducting fluid until charge destabilizes the fluid meniscus resulting in ejection of drops. Even at a constant voltage, the fluid pulsates because of oscillation between charge buildup and drop ejection. In this continuous-DC mode, there is little control over the drop size or their ejection frequency (Jayasinghe et al., 2002; Wang et al., 2005). In some cases, drop ejection is nearly random and reliable printing cannot be achieved. A pulsed DC affords greater flexibility in controlling drop size and ejection interval (Kim et al., 2006; Lee et al., 2008; Mishra et al., 2010; Paine, 2009; Paine et al., 2007). After drop ejection, charge around the nozzle tip is decreased and surface-tension forces dominate; the meniscus pulls back when there is little charge. When the next voltage pulse is applied, the electrostatic force dominates and another drop is ejected.

The amplitude and the duration of the applied voltage are the primary parameters that affect the characteristics of the inkjet. The product of amplitude and duration of the pulsed voltage yields the total amount of charge supplied. Thus, in theory, charge density from a low-amplitude, long-duration voltage pulse would have the same effect as a high-amplitude, short-duration voltage pulse; however, they are quite different in practice.

If the voltage-pulse duration is too long, spindle, string-jet, or spray modes appear. Conversely, if duration is too short, ejection may not occur. Xu et al. (2011) showed the effect of amplitude variation with fixed-duty-cycle-ratio (which is referred to as "duration" in this paper); the supplied volume of liquid is proportional to the product of deposition frequency and the cube of the drop diameter ($Q \propto f_{dep} D_{dep}^3$).

Here we report comprehensive experimental data that describe how the EHD inkjet ejection mode changes with variation in the amplitude or duration of the applied voltage pulse. The ranges of amplitude and duration that yield the microdrippng mode (which is desirable for fine printing) are identified. These results delineate a map of the various modes and it can be used as a guideline for EHD inkjet operators.

2. Experimental setup

Fig. 1 is a schematic of the experimental setup for the EHD printing system. Liquid is supplied to the stainless-steel nozzle (EFD, 18 gage, inner and outer diameters of 0.84 and 1.27 mm, respectively) by a syringe pump (KDS 100). A multi-function synthesizer (NF Corporation, WF 1973) generates a step-function signal, which is sent to the HV-amplifier (TREK 10/40A) for thousand-fold amplification. The amplified signal (voltage) is supplied to the conducting needle, which is directly connected to the syringe pump. A high-speed camera (Vision Research, Inc., Phantom 7.3) with zoom lens (1.56 μm/pixel) and Halogen lamp (250 W) captures magnified images of ejected ink drops. Snapshots are taken at 100-μs interval. The motorized stage holding the substrate (Future Science, FS-XY-0.1-100) can maneuver up to a maximum distance of 100 mm in 0.1-μm increments. The distance between the nozzle tip and the well-polished copper substrate is fixed at 5 mm. The working fluid is diethylene glycol (DEG) whose thermo-physical properties are summarized in Table 1. All measurements for pulse duration and applied voltage contained errors less than 5% based on repeatability tests.

3. Results and discussion

3.1. Effect of duration

Fig. 2 shows the effect of pulse duration on the inkjet mode when $f=1$ Hz (one drop per second), $V=8.7$ kV, and $Q=0.2$ ml/h. The duration, τ, has been varied from 1 to 500 ms; voltage is applied for a half second per cycle when τ is 500 ms. Of course, duration must always be less than inverse frequency or pulsation is not possible.

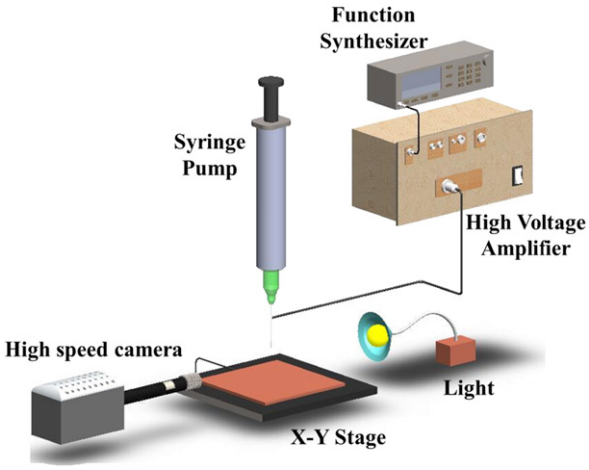

Fig. 1. Schematic of the experimental setup for the EHD printing system.

Table 1
DEG properties.

Molecular weight, MW (g/mol)	106.12
Density, ρ (kg/m^3)	1118
Surface tension, σ (mN/m)	44.8
Viscosity, μ (mPa s)	38.5
Electrical conductivity, K (μS/cm)	0.24
Electrical permittivity, ε	6.66
Boiling point, T_b (°C)	244

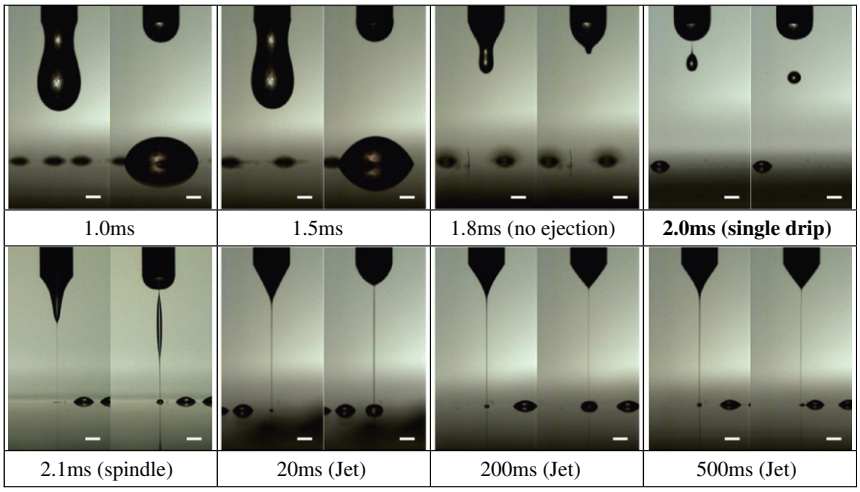

Fig. 2. Effect of the pulse duration on microdripping and jet modes. The operating conditions are $f=1$ Hz, $V=8.7$ kV, and $Q=0.2$ ml/h (Scale bar=500 μm).

From Fig. 2, when duration is short (i.e., $\tau \leq 1.5$ ms), bulky pendant dripping due to gravity appears because of lack of electrostatic charge. When $\tau=1.8$ ms, influence of the electrostatic charges begins to manifest, but the duration is still insufficient to yield DOD. When $\tau=2.0$ ms, microdripping begins, but it quickly transitions into a spindle mode when duration is slightly increased to $\tau=2.1$ ms. This indicates that the desirable microdripping mode has a narrow stability range. Further increase in duration yields the jet mode; drops are not generated. Despite $f=1$ Hz, multiple larger parcels of fluid connected by thin streams of fluid are ejected per second because the fluid is overloaded with charge and electrostatic repulsion overcomes the surface tension and viscous forces. When duration is further increased to $\tau=500$ ms, the additional charge can atomize the fluid, often forming a spray. This yields many drops of various sizes deposited on the substrate. Poor printing results; variously sized drops are randomly deposited around the target location on the substrate.

3.2. Effect of voltage amplitude

Fig. 3 shows the effect of voltage amplitude on the inkjet mode when $f=1$ Hz, $\tau=2$ ms, and $Q=0.2$ ml/h. Here, the voltage amplitude ranges from 8.6 kV to 10 kV. It was previously determined that optimal microdripping is achieved when $\tau=2$ ms and V is between 8.7 and 8.8 kV for $f=1$ Hz. Below 8.7 kV, no drop is ejected at $\tau=2$ ms. Upon further increasing the voltage, the drop is stretched before detachment yielding multiple necks that eventually break up into satellite droplets; see the snapshot at $V=8.9$ kV in Fig. 3. At $V=9.0$ kV, the stretched fluid column thickens and the inkjet enters a spindle mode. For $V \geq 9.3$ kV, there is sufficient charge to yield a Taylor cone jet. However, this cone jet also pulsates with a frequency related to the voltage duration of $\tau=2$ ms. When the fluid is not charged, the cone jet retracts due to surface tension. The resulting phenomenon is shown in Fig. 3 for $V \geq 9.3$ kV.

Fig. 4 summarizes the results from Figs. 2 and 3 with data plotted as a function of nondimensional duration (τ^*) and amplitude (V^*) of the applied voltage. Four modes are identified: microdripping, spindle, (string) jet, and spray modes. This map applies to data collected at $f=1$ Hz and $Q=0.2$ ml/h using a nozzle diameter of $d_n=1.27$ mm with DEG as the working fluid. If frequency increases, microdripping, delineated by the red squares, would shift to the upper right region because higher frequencies require increased voltage to yield stable dots. Fig. 4 shows that even small deviations from the microdripping line shift to the poor-ejection mode (toward the left) or to the spindle mode (toward the right). Apparently, the microdripping mode has a small window of stability for pulse duration (τ) and voltage (V). The microdripping mode shows an inverse relationship between τ and V; as τ increases, the voltage needs to decrease. This inverse relationship applies for ranges of $4 \times 10^{-5} < \tau^* < 15 \times 10^{-5}$ and $1.1 \times 10^{-3} < V^* < 1.5 \times 10^{-3}$. Excess voltage yields either the jet or spray mode depending on τ^*. The jet mode appears at the lower voltage range and the spray mode at the upper end. The

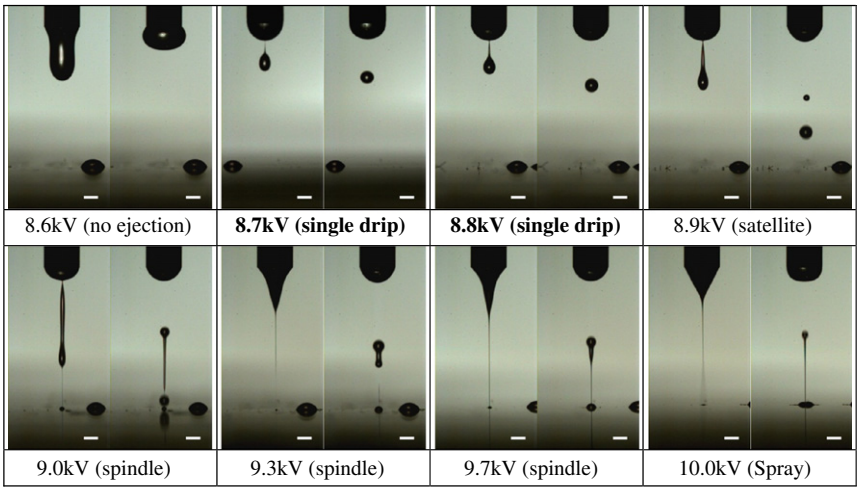

Fig. 3. Effect of the voltage amplitude on microdripping and jet modes. The operating conditions are $f=1$ Hz, $\tau=2.0$ ms, and $Q=0.2$ ml/h (Scale bar$=500$ μm).

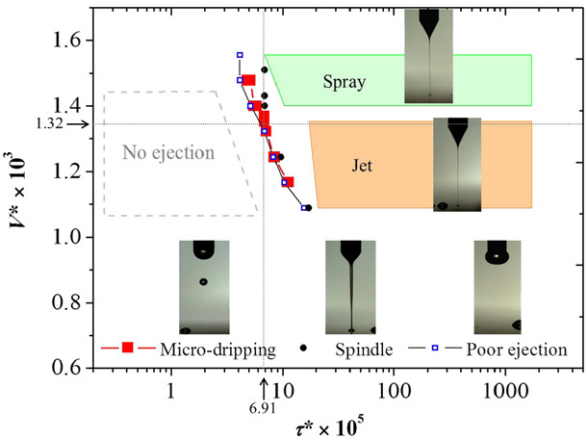

Fig. 4. Regime identification map for various inkjet modes ($f=1$ Hz). The dimensionless duration and voltage are defined as $\tau^*=\tau(U/d_n)$ and $V^*=(V^2\varepsilon_0)/(\sigma d_n)$, where U and d_n are the jet speed and nozzle diameter, respectively. ε_0 and σ are the permittivity of free space and surface tension. The values of $\tau^*=6.91\times10^{-5}$ and $V^*=1.32\times10^{-3}$ correspond to $\tau=2$ ms and $V=8.7$ kV, respectively, when using $U=4.39\times10^{-5}$ m/s, $d_n=1.27$ mm, $\varepsilon_0=8.85\times10^{-12}$ C^2/N-m^2, and $\sigma=44.8$ mN/m.

higher the voltage, the easier it is to atomize the fluid that leads to spray formation. It is noted that there is no ejection regardless of voltage if the duration is short (i.e., $\tau^*<4\times10^{-5}$).

3.3. *Effect of frequency*

Drop size control for an EHD DOD inkjet can be achieved by tuning the frequency of the pulsed-DC voltage. Frequency is defined as the number of drops ejected per second and high-speed printing requires a correspondingly high frequency. However, in reality, the drop generation rate is (much) less than the pulsed DC frequency when $f>60$ Hz. High DC voltage frequencies are not perfectly reflected in the drop generation rate because the liquid is imperfectly conducting and has non-zero viscosity.

Kang et al. (2011) demonstrated consistency between the drop generation rate and pulsing frequency for $f\leq10$ Hz. Here, we extend this to $f\leq30$ Hz, which is comparable to the frequency observed by Mishra et al. (2010) For $f>60$ Hz, there is increased departure of the drop-generation rate from the voltage frequency, which was confirmed by counting the number of drops printed on the substrate per second.

Fig. 5 shows the effect of pulsed frequency on drop size in the range of $1<f<30$ Hz during the microdripping mode at $V=8.7$ kV, and $Q=0.2$ ml/h. The higher the frequency, the smaller the drop size. This is the true drop-on-demand because the drop size can be controlled by tuning the pulsing frequency. The drop size at $f=30$ Hz is around 135 μm. The smallest drop size observed at higher frequencies was about ~50 μm (not shown here).

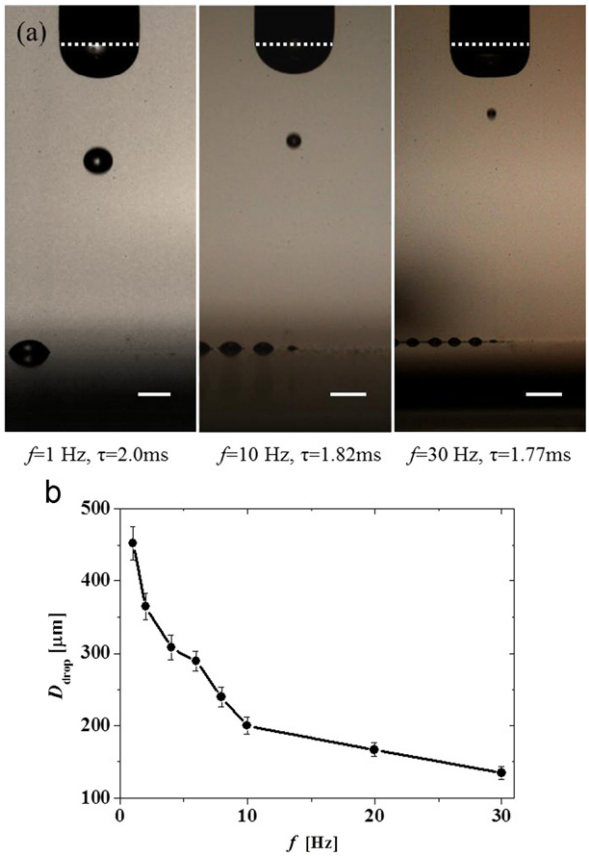

Fig. 5. Effect of the pulsing frequency during the microdripping mode. The operating conditions are $V=8.7$ kV and $Q=0.2$ ml/h (Scale bar=500 μm). (a) Snapshots, (b) effect of voltage frequencies on the drop size.

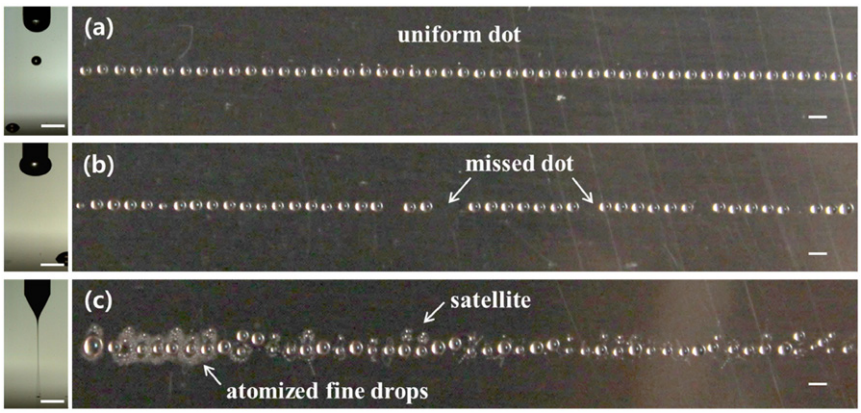

Fig. 6. Dot-printing at $f=1$ Hz and $Q=0.2$ ml/h. (a) Optimized microdripping; uniform dot priting is achieved when $V=8.7$ kV and $\tau=2.0$ ms. (b) Poor-ejection occurs when duration is short; $V=8.7$ kV and $\tau=1.8$ ms. (c) Jet (or spray) mode is due to excessive charge and pulse duration ($V=10.0$ kV and $\tau=5.0$ ms); atomized droplets are randomly scattered around the inkjet dots. (Scale bar=1 mm).

Fig. 6 shows the printed DEG dots on a stainless steel substrate during (a) the microdripping mode, (b) the poor-ejection mode, and (c) the spray mode for operating conditions of $f=1$ Hz and $Q=0.2$ ml/h. During microdripping, uniform dots are generated and they are line-printed on the substrate. During the poor-ejection mode, a slight decrease in τ varies the targeting angle and the printed line is not straight. The spray mode yields irregularly shaped drops surrounded by atomized droplets.

4. Conclusions

Comprehensive experimental data that describe how the EHD inkjet ejection mode changes with variation in the amplitude or duration (or duty cycle or relaxation time, τ) of the applied voltage pulsing frequency of $f=1$ Hz have been reported. Four modes are identified: microdripping, spindle, (string) jet, and spray modes. If the voltage-pulse duration is too long, spindle, string-jet, or spray modes appear. Conversely, if duration is too short, ejection may not occur. The ranges of amplitude and duration that yield the microdrippng mode (which is desirable for fine printing) are identified. Apparently, the microdripping mode has a small window of stability for pulse duration (τ) and voltage (V). These results delineate a map of the various modes and it can be used as a guideline for EHD inkjet operators.

Acknowledgment

This work was supported by the Center for Inorganic Photovoltaic Materials NRF-2011-0007182 and 2010-0010217 funded by the Korean government (MEST). This research was also supported by the Converging Research Center Program through the Ministry of Education Science and Technology (2010K000969). This work was also supported by the Human Resources Development of the Korea Institute of Energy Technology Evaluation and Planning (KETEP) grant funded by the Ministry of Knowledge Economy, Republic of Korea (No. 20104010100640).

References

Eom, S.H., Senthilarasu, S., Uthirakumar, P., Hong, C.H., Lee, Y.S., & Lim, J.S., et al. (2008). Preparation and characterization of nano-scale ZnO as a buffer layer for inkjet printing of silver cathode in polymer solar cells. *Solar Energy Materials and Solar Cells*, *92*, 564–570.

Eom, S.H., Senthilarasu, S., Uthirakumar, P., Yoon, S.C., Lim, J.S., & Lee, C.J., et al. (2009). Polymer solar cells based on inkjet-printed PEDOT:PSS layer. *Organic Electronics*, *2009*, 536–542.

Ishida, Y., Nakagawa, G., & Asano, T. (2007). Inkjet printing of nickel nanosized particles for metal-induced crystallization of amorphous silicon. *Japanese Journal of Applied Physics*, *46*, 6437–6443.

Jaworek, A., & Sobczyk, A.T. (2008). Electrospraying route to nanotechnology: an overview. *Journal of Electrostatics*, *66*, 197–219.

Jayasinghe, S.N., Edirisinghe, M.J., & Wilde, T.D. (2002). A novel ceramic printing technique based on electrostatic atomization of a suspension. *Materials Research Innovations*, *6*, 92–95.

Kang, D.K., Lee, M.W., Kim, H.Y., James, S.C., & Yoon, S.S. (2011). Electrohydrodynamic pulsed-inkjet characteristics of various inks containing aluminum particles. *Journal of Aerosol Science*.

Kim, D.J., Jeong, S.H., Park, B.K., & Moon, J.H. (2006). Direct writing of silver conductive patterns: improvement of film morphology and conductance by controlling solvent compositions. *Applied Physics Letters*, *89*, 264101.

Krebs, F.C. (2009). Polymer solar cell modules prepared using roll-to-roll methods: knife-over-edge coating, slot-die coating and screen printing. *Solar Energy Materials & Solar Cells*, *93*, 465–475.

Lee, S.H., Byun, D.Y., Jung, D.W., Choi, J.Y., Kim, Y.J., & Yang, J.H., et al. (2008). Pole-type ground electrode in nozzle for electrostatic field induced drop-on-demand inkjet head. *Sensors and Actuators A*, *141*, 506–514.

Mishra, S., Barton, K.L., Alleyne, A.G., Ferreira, P.M., & Rogers, J.A. (2010). High-speed and drop-on-demand printing with a pulsed electrohydrodynamic jet. *Journal of Micromechanics and Microengineering*, *20*, 095026–095033.

Paine, M.D. (2009). Transient electrospray behaviour following high voltage switching. *Microfluid Nanofluid*, *6*, 775–783.

Paine, M.D., Alexander, M.S., Smith, K.L., Wang, M., & Stark, J.P.W. (2007). Controlled electrospray pulsation for deposition of femtoliter fluid droplets onto surfaces. *Journal of Aerosol Science*, *38*, 315–324.

Salata, O.V. (2005). Tools of nanotechnology: electrospray. *Current Nanoscience*, *1*, 25–33.

Singh, M., Haverinen, H.M., Dhagat, P., & Jabbour, G.E. (2010). Inkjet printing—process and its applications. *Advanced Materials*, *22*, 673–685.

Wang, D.Z., Jayasinghe, S.N., & Edirisinghe, M.J. (2005). High resolution print-patterning of a nano-suspension. *Journal of Nanoparticle Research*, *7*, 301–306.

Wu, N., Pease, L.F., & Russel, W.B. (2006). Toward large-scale alignment of electrohydrodynamic patterning of thin polymer films. *Advanced Functional Materials*, *16*, 1992–1999.

Wu, N., & Russel, W.B. (2009). Micro- and nano-patterns created via electrohydrodynamic instabilities. *Nano Today*, *4*, 180–192.

Xu, L., Wang, X., Lei, T., Sun, D., & Lin, L. (2011). Electrohydrodynamic deposition of polymeric droplets under low-frequency pulsation. *Langmuir*

Yurteri, C.U., Hartman, R.P.A., & Marijnissen, J.C.M. (2010). Producing pharmaceutical particles via electrospraying with an emphasis on nano and nano structured particles—a review. *KONA Powder and Particle Journal*, *28*, 91–115.